nature chemical biology

Two interconverting Fe(IV) intermediates in aliphatic chlorination by the halogenase CytC3

Danica P Galonić[1], Eric W Barr[2], Christopher T Walsh[1], J Martin Bollinger, Jr[2,3] & Carsten Krebs[2,3]

Enzymatic incorporation of a halogen atom is a common feature in the biosyntheses of more than 4,500 natural products[1–5]. Halogenation of unactivated carbon centers in the biosyntheses of several compounds of nonribosomal peptide origin is carried out by a class of mononuclear nonheme iron enzymes that require α-ketoglutarate (αKG, 1), chloride and oxygen[6]. To investigate the ability of these enzymes to functionalize unactivated methyl groups, we characterized the chlorination of the γ-methyl substituent of L-2-aminobutyric acid (L-Aba, 2) attached to the carrier protein CytC2 by iron halogenase (CytC3) from soil *Streptomyces* sp. We identified an intermediate state comprising two high-spin Fe(IV) complexes in rapid equilibrium. At least one of the Fe(IV) complexes abstracts hydrogen from the substrate. The demonstration that chlorination proceeds through an Fe(IV) intermediate that cleaves a C-H bond reveals the mechanistic similarity of aliphatic halogenases to the iron- and αKG-dependent hydroxylases.

Halogenation in natural product biosynthesis occurs on a diverse array of scaffolds, including olefinic centers, electron-rich aromatic substrates and unactivated aliphatic carbon centers[7]. Because of the difficulties associated with the functionalization of unactivated alkyl groups, these halogenations represent a substantial chemical challenge. A class of halogenating enzymes (halogenases) responsible for chlorination of alkyl side chains of amino acids during the biosynthesis of several natural products of nonribosomal peptide origin has recently been characterized[6,8,9]. Halogen incorporation follows nonribosomal peptide biosynthetic logic: initial activation of the amino acid by an adenylation (A) domain is followed by its loading on the phosphopantetheinyl arm of the thiolation (T) module. The resultant aminoacyl-*S*-T protein is the substrate for the halogenase, which chlorinates an unactivated methyl group of the tethered amino acid. For example, chlorination of the γ-methyl group of L-threonine (3) tethered to the A-T didomain protein SyrB1 by the halogenase SyrB2 produces 4-chloro-L-threonine-*S*-SyrB1, an intermediate in the biosynthesis of syringomycin (4)[6]. CytC3, the halogenase isolated from soil *Streptomyces* sp., chlorinates the γ-methyl group of L-Aba or L-valine (5) tethered to the carrier protein CytC2 (ref. 10). The tandem action of two halogenases, BarB1 and BarB2, effects the triple chlorination of the side chain methyl group of L-leucine-*S*-BarA in barbamide (6) biosynthesis[8]. Finally, γ-chlorinated L-*allo*-isoleucine (7), which is generated by an analogous halogenation, is an intermediate in the formation of the cyclopropane ring of the *Pseudomonas syringae* natural product coronamic acid (8)[9].

Earlier studies showed that the *in vitro* reconstitution of the aliphatic halogenation activity of these enzymes requires halogenase, Fe(II) and three small-molecule cosubstrates: αKG, oxygen and chloride[6]. However, the mechanism of such aliphatic halogenations has not been elucidated. The requirement for Fe(II), αKG and oxygen is similar to that of the Fe(II)- and αKG-dependent dioxygenases, which comprise arguably the largest and functionally most diverse group of mononuclear nonheme iron enzymes[11–13]. They reductively activate molecular oxygen, cleave their cosubstrate (αKG) to CO_2 and succinate (9), and oxidize carbon centers in their substrates by two electrons[11–14].

The central feature of investigations of this class of αKG-dependent oxygenases has been the prediction and subsequent experimental verification of a high-valent Fe(IV)-oxo complex as the oxidant that effects homolysis of unactivated C-H bonds in substrates before OH rebound[14]. The prototype has become taurine (10)–αKG dioxygenase (TauD), in which two iron-containing intermediates were detected by stopped-flow (SF) absorption and freeze-quench (FQ) Mössbauer spectroscopies[15]. The first intermediate has an Fe(IV) center in the unusual high-spin ($S = 2$) configuration[15]. The large kinetic isotope effect ([^{2}H] KIE) on its decay ($k_H/k_D \sim 50$) in the presence of deuterated substrate identified this intermediate as the species that cleaves the C-H bond[16,17]. Subsequent resonance Raman[18] and X-ray absorption spectroscopic[19] experiments confirmed that it contains an Fe(IV)-oxo group. The second accumulating state is an Fe(II)-containing TauD–products complex[20]. Prolyl-4-hydroxylase (P4H) also generates such intermediates[21].

Insight into the catalytic strategy of Fe(II)- and αKG-dependent halogenases came from the crystal structure of the syringomycin halogenase SyrB2 (ref. 22). In contrast to the αKG-dependent dioxygenases, in which the Fe(II) center is coordinated by three amino acid residues known as the $(His)_2(Asp/Glu)$ "facial triad"[23], the iron center of SyrB2 is coordinated by only two histidine residues, and the typical carboxylate from the protein is replaced by an exogenous chloride ligand. From this insight, the mechanism shown in **Scheme 1** was

[1]Department of Biological Chemistry and Molecular Pharmacology, Harvard Medical School, 240 Longwood Ave., Boston, Massachusetts 02115, USA. [2]Department of Biochemistry and Molecular Biology and [3]Department of Chemistry, The Pennsylvania State University, University Park, Pennsylvania 16802, USA. Correspondence should be addressed to C.K. (ckrebs@psu.edu), J.M.B. (jmb21@psu.edu) or C.T.W. (christopher_walsh@hms.harvard.edu).

Received 21 August 2006; accepted 13 December 2006; published online 14 January 2007; doi:10.1038/nchembio856

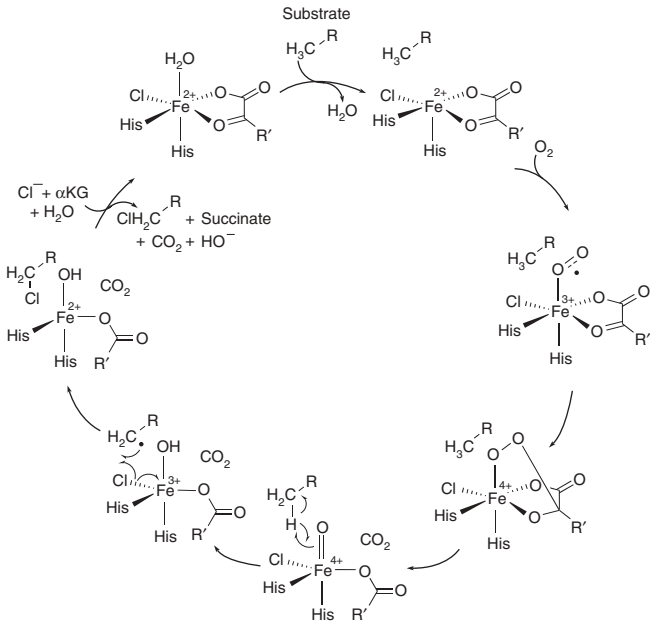

Scheme 1 Proposed mechanism of the Fe(II)- and αKG-dependent halogenases. R = –CH_2–L–CH(NH_2)–CO–*S*-CytC2; R′ = –$(CH_2)_2CO_2^-$.

proposed[7,22]. The key postulated intermediate is a ClFe(IV)-oxo complex that activates the substrate by hydrogen atom abstraction to yield a ClFe(III)-OH complex and a substrate radical. Substrate chlorination then proceeds via "rebound" of a chloride radical, rather than the hydroxyl radical rebound postulated for hydroxylases. Herein we provide kinetic and spectroscopic evidence for the ClFe(IV)-oxo complex in the streptomycete aliphatic halogenase CytC3.

We chose the aliphatic halogenation system isolated from the cytotrienin (**11**)-producing *Streptomyces* sp. as ideal for testing the proposed mechanism by direct characterization of intermediates. The system consists of three proteins: CytC1, CytC2 and CytC3. CytC1 is an adenylation protein that selects and activates L-2-aminobutyrate and installs it in thioester linkage on the thiolation domain (CytC2), where it is acted on by the halogenating enzyme CytC3 (**Supplementary Scheme 1** online). Previous studies demonstrated that apo-CytC2 (11.4 kDa) can be obtained in high yields and then quantitatively appended with the phosphopantetheine arm by incubation with coenzyme A (**12**) and the phosphopantetheinyl transferase Sfp[24]. Furthermore, the holoprotein so obtained can be quantitatively loaded with L-Aba via incubation with CytC1 and ATP (**13**). The resulting L-Aba-*S*-CytC2 is a substrate for the halogenase CytC3 (36.7 kDa)[10].

Addition of Fe(II) to an anaerobic solution of L-Aba-*S*-CytC2 and CytC3 in the presence of αKG and Cl^- resulted in development of the typical Fe(II)-to-αKG charge-transfer band (λ_{max} = 520 nm, $\varepsilon_{520} \sim 220\ M^{-1}\ cm^{-1}$, **Fig. 1**)[25]. The plot of A_{520} versus [Fe(II)] (**Fig. 1a**) indicates a very low effective $K_{d,\ Fe(II)}$ and a binding stoichiometry of 0.8 equivalents of Fe(II).

Absorbance changes upon reaction of the CytC3–Fe(II)–αKG–Cl^-–L-Aba-*S*-CytC2 complex with oxygen-saturated buffer at 5 °C revealed the accumulation of an intermediate state. An absorption feature centered at 318 nm developed rapidly and then decayed (**Fig. 1b**; formation rate constant = 18 s^{-1}, decay rate constant = 0.20 s^{-1}). The similarity of these observations to changes previously attributed to formation and decay of Fe(IV)-oxo intermediates in TauD[16] and P4H[21] suggests the accumulation of such a species in the CytC3 reaction. The ΔA_{520}-versus-time trace (**Fig. 1b**) also has two distinct kinetic phases, which correlate with those observed for ΔA_{318}. In the first phase, ΔA_{520} increases minimally, suggesting that the 318-nm-absorbing intermediate also absorbs substantially at 520 nm, thereby compensating for the loss of the starting complex. The loss of absorption at 520 nm during the second phase suggests accumulation of a second state that has little or no absorption at 520 nm—presumably an Fe(II)–product(s) complex, in analogy to TauD[20].

The possibility that the intermediate absorbing at 318 nm effects hydrogen atom abstraction was assessed by using L-*4,4,4-d*$_3$-Aba-*S*-CytC2 as the substrate and testing for a [^{2}H] KIE on decay of the intermediate. The ΔA_{318} kinetic trace for the reaction of the CytC3–Fe(II)–αKG–Cl^-–L-*4,4,4-d*$_3$-Aba-*S*-CytC2 complex with O_2 (**Fig. 1b**) under conditions identical to those described above differs markedly from the trace for the reaction with unlabeled substrate (**Fig. 1b**). Whereas the rise phases are essentially coincident, the deuterated substrate delays the decay of A_{318} so markedly that the absorbance becomes stable for at least 10 s (**Fig. 1b**). This large [^{2}H] KIE implies that the associated intermediate abstracts hydrogen to initiate chlorination.

To test the expectation that the absorbance change at 318 nm is associated with the postulated Fe(IV)-oxo intermediate, FQ Mössbauer experiments were carried out under identical reaction conditions (**Fig. 2**). The CytC3–Fe(II)–αKG–Cl^-–L-Aba-*S*-CytC2 complex showed a quadrupole doublet (**Fig. 2a**) with parameters (isomer shift, δ, of 1.19 mm s^{-1}; quadrupole splitting parameter, $|\Delta E_Q|$, of 2.75 mm s^{-1}) characteristic of high-spin Fe(II). Spectra of samples freeze-quenched after mixing of the complex with O_2 (**Fig. 2a**) showed two new peaks at 0.58 mm s^{-1} and 0.85 mm s^{-1}, which implies formation of (at least) two new species upon reaction with O_2. Analysis of the spectrum of the new state (**Fig. 2b**), which was obtained by removal of the contribution of the reactant complex, reveals the presence of two sharp (line width = 0.26 mm s^{-1}) quadrupole doublets with similar parameters: δ_1 = 0.30 mm s^{-1} and $|\Delta E_{Q1}|$ = 1.09 mm s^{-1}; δ_2 = 0.22 mm s^{-1} and $|\Delta E_{Q2}|$ = 0.70 mm s^{-1}. These parameters, in particular δ_1 and ΔE_{Q1}, are similar to values for the Fe(IV)-oxo intermediates in TauD and P4H. The value of δ_2, although lower, is still in the range typical of the Fe(IV) oxidation state. The ratio of the two Fe(IV) complexes in the reaction was approximately 4:5. Importantly, spectra of samples frozen at different reaction times show that the ratio of the

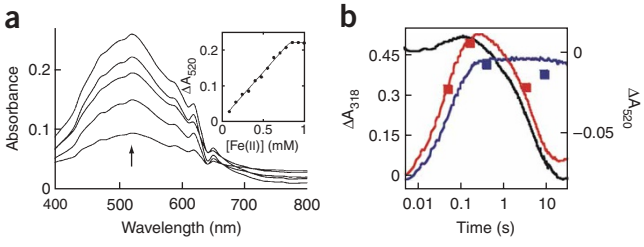

Figure 1 Absorption spectroscopy of CytC3. (**a**) Titration of Fe(II) into a solution of the CytC3–αKG–Cl^-–L-Aba-*S*-CytC2 complex. The spectra shown correspond to Fe(II) concentrations of (from bottom to top) 160 μM, 390 μM, 540 μM, 700 μM and 840 μM. The points in the inset depict the change of absorbance at 520 nm. (**b**) SF absorption kinetic traces. The reaction of CytC3–Fe(II)–αKG–Cl^-–L-Aba-*S*-CytC2 with O_2 monitored at 318 nm (red trace) and 520 nm (black trace), and the reaction of CytC3–Fe(II)–αKG–Cl^-–L-*4,4,4-d*$_3$-Aba-*S*-CytC2 with O_2 monitored at 318 nm (blue trace). The red and blue squares represent the sum of concentrations of the two Fe(IV) complexes obtained by FQ Mössbauer analysis of samples prepared under identical reaction conditions.

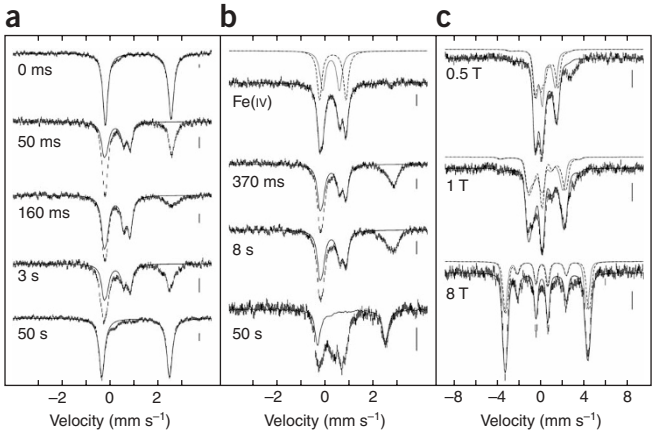

Figure 2 Mössbauer spectroscopy of CytC3. (**a**,**b**) 4.2 K/zero-field spectra of samples frozen after mixing the reactant complex, prepared with either unlabeled (**a**) or deuterated (**b**) substrate with O_2. The deduced spectrum of the Fe(IV) complexes is also shown (**b**, top). Reaction times are indicated at the spectra. Solid lines in the left panel of the 0 s and 50 s spectra are simulations of the reactant and product(s) complexes, respectively. All other solid lines represent the two Fe(IV) intermediates. The dashed and dotted lines above the reference spectrum are the individual contributions of the two Fe(IV) complexes. Simulation parameters are given in the text. (**c**) 4.2 K/variable-field spectra of the two Fe(IV) complexes. The magnetic field strength is indicated at the spectra. Simulation parameters: zero-field splitting $D_1 = D_2 = 8.1$ cm^{-1}; rombicities $(E/D)_1 = (E/D)_2 = 0.02$; asymmetry parameters $\eta_1 = \eta_2 = 0$; hyperfine couplings $A_{x,y,1}/g_N\beta_N = A_{x,y,2}/g_N\beta_N = -18.0$ T, isomer shift $\delta_1 = 0.30$ mm s^{-1}, quadrupole splitting parameter $\Delta E_{Q1} = -1.09$ mm s^{-1}, isomer shift $\delta_2 = 0.22$ mm s^{-1} and quadrupole splitting parameter $\Delta E_{Q2} = -0.70$ mm s^{-1}. The individual contributions of the two sites are shown as dashed and dotted lines. The vertical bar on the right side of each spectrum indicates 0.2% absorption.

two Fe(IV) complexes is (within experimental error) unchanged with time, which suggests that the two Fe(IV) intermediates are in a rapid equilibrium. The total quantity of the Fe(IV) intermediates (determined by Mössbauer spectroscopy) (**Fig. 1b**) compared to ΔA_{318} demonstrates that the spectroscopic features are kinetically correlated. For this comparison we assumed that the molar absorptivity for the Fe(IV) intermediate state is 1,500 M^{-1} cm^{-1}, which is the value determined for the Fe(IV)-oxo intermediates in both TauD and P4H[15,21].

The spectrum of the 50 s sample (**Fig. 2a**) reveals that both Fe(IV) intermediates have completely decayed by this reaction time. Most of the intensity of this spectrum (95%) is contributed by a quadrupole doublet with parameters typical of high-spin Fe(II) ($\delta = 1.09$ mm s^{-1} and $|\Delta E_Q| = 2.83$ mm s^{-1}). These parameters are distinct from those of the reactant complex, which suggests that a different state of the catalytic cycle has accumulated. Analogy to previous results for TauD and P4H suggests that this second state is most likely a product(s) complex.

The [^{2}H] KIE implied by the SF absorption data was confirmed by FQ Mössbauer experiments with L-*4,4,4-d*$_3$-Aba-*S*-CytC2 as the substrate (**Fig. 2b**). The peaks of both Fe(IV) intermediates appear in approximately the same ratio (4:5) as that seen with the unlabeled substrate. The sum of their contributions remains nearly unchanged from 370 ms to 8 s (69% and 63%, respectively), thereby providing independent evidence for a large [^{2}H] KIE. Moreover, the total amount of the Fe(IV) complexes again correlates well with the ΔA_{318} data (**Fig. 1b**). The spectrum of the 50 s sample with deuterated substrate shows clear differences compared with the spectrum of the 50 s sample with unlabeled substrate. In addition to the peaks associated with the high-spin Fe(II) product(s) complex observed in the spectrum of the 50 s sample with unlabeled substrate (33% of total intensity), the spectrum shows intense but featureless absorption between 0 and 1 mm s^{-1}, which we attribute to products of the unproductive decay of the Fe(IV) complexes and possibly the remaining Fe(IV) intermediates. However, given the lack of resolution of the spectrum, it is not possible to quantify the various contributing components.

Mössbauer spectra of the Fe(IV) complexes acquired in external magnetic fields provide further insight into their electronic structure (**Fig. 2c**; the contribution of the reactant complex has been removed from the spectra). The spectra resemble those observed for the Fe(IV)-oxo intermediates in TauD[15,26] and P4H[21], as well as that of the $(H_2O)_5$Fe(IV)-oxo complex (**14**)[27], and they demonstrate that both Fe(IV) complexes have a nearly axial $S = 2$ ground state, an axial ^{57}Fe A-tensor, and a small, negative quadrupole splitting. Spectral simulations according to the spin-Hamiltonian formalism for an $S = 2$ spin system in the slow relaxation limit are shown in **Figure 2**.

The demonstration that chlorination of the side chain methyl group of CytC2-tethered L-Aba proceeds through Fe(IV) intermediates that cleave the C-H bond underscores the mechanistic similarity of the halogenases to previously characterized αKG-dependent dioxygenases. This similarity suggests that halogenation may have evolved from hydroxylation activity simply by loss of the iron-coordinating carboxylate ligand, which would allow for coordination of exogenous chloride and its subsequent transfer to the substrate radical during catalysis. The extremely slow decay of the Fe(IV) complexes in the presence of deuterated substrate suggests that the active site of the halogenase is quite effective at suppressing side reactions of the high-valent intermediates, which in related enzyme systems are believed to effect self-hydroxylation of adjacent tyrosine residues[28,29].

The demonstration of two interconverting Fe(IV) complexes in CytC3 contrasts with the single Fe(IV)-oxo complex detected in each of the dioxygenases. Because characteristics of the electronic ground states of both complexes conform to those observed experimentally[27] and rationalized computationally[30] for Fe(IV)-oxo complexes, we speculate that they both contain an oxo ligand and represent two distinct conformers in rapid equilibrium. Spectroscopic verification of this assignment (for example, by X-ray absorption spectroscopy) may be complicated by the presence of nearly equal amounts of two distinct complexes. Attempts to enrich one of the two Fe(IV) complexes by altering the reaction conditions (for example, changing [Cl$^-$], using an alternative substrate, or using D_2O as solvent) were unsuccessful (**Supplementary Fig. 1** online).

The mechanistic studies presented herein support the postulated catalytic mechanism of Fe(II)- and αKG-dependent halogenases (**Scheme 1**). The early steps of the mechanism leading to the ClFe(IV)-oxo complex, which is the species proposed to abstract the hydrogen atom from the substrate, are likely conserved among the dioxygenases and halogenases. After hydrogen atom abstraction, the ClFe(III)-OH species could transfer either a hydroxyl radical or a chlorine atom to the substrate radical. So far, efforts to detect hydroxylation of the loaded amino acid by the aliphatic halogenases have failed[6,8–10], which indicates a strong preference for the Cl$^\bullet$ rebound. The exclusive selectivity for halogenation has also been observed in the model systems in which iron is coordinated by both hydroxide and chloride ligands[31]. An analogous preference for transfer of a ligand other than hydroxyl (thiyl) has been observed in the reaction of isopenicillin *N* synthase with its native substrate[32]. In addition, it is likely that the αKG-dependent halogenases control the

radical rebound outcome by proper positioning of the substrate in the active site. Ongoing efforts to obtain further insight into the geometric and electronic structures of the CytC3 Fe(IV) complexes may help to rationalize the divergent reactivities of the halogenases and dioxygenases.

METHODS

Chemical synthesis. Preparation of L-2-amino-*4,4,4-d*$_3$-butyric acid (L-*4,4,4-d*$_3$-Aba,15) is described in **Supplementary Methods** online.

Substrate preparation. CytC1, CytC2 and CytC3 were overproduced and purified as previously described[10]. We post-translationally modified the thiolation domain protein CytC2 with the phosphopantetheinyl group by using the purified Sfp protein[24], generating the holo-CytC2. We prepared L-Aba-*S*-CytC2 and L-*4,4,4-d*$_3$-Aba-*S*-CytC2 by incubation of holo-CytC2 (431 μM) with either L-Aba or L-*4,4,4-d*$_3$-Aba (7.2 mM) in the presence of CytC1 (44 μM), $MgCl_2$ (18 mM) and ATP (10.8 mM) in 100 mM HEPES, pH 7.5, at 23 °C for 1.5 h. Then we concentrated (to 5–5.5 mM) and deoxygenated the obtained amino acid–loaded CytC2.

SF absorption and FQ Mössbauer experiments. We mixed deoxygenated buffered (100 mM HEPES, pH 7.5) solutions of CytC3, L-Aba-*S*-CytC2, sodium chloride and αKG in an anaerobic glove box and then added an Fe(II) solution (20 mM $Fe(NH_4)_2(SO_4)_2$ for SF and 100 mM ^{57}Fe for FQ experiments) into the cooled (5 °C) protein solution in the absence of oxygen (final concentrations: [CytC3] = 1 mM, [αKG] = 4.8 mM, [Cl^-] = 48 mM, [Fe(II)] = 0.8 mM, [L-Aba-*S*-CytC2] = 2.2 mM). Then we mixed the resulting CytC3–Fe(II)–αKG–Cl^-–L-Aba-*S*-CytC2 solution at 5 °C with a buffered (100 mM HEPES, pH 7.5) solution saturated with O_2 in 1:1 ratio. We carried out analogous experiments with L-*4,4,4-d*$_3$-Aba-*S*-CytC2. We performed spectroscopic experiments as previously described[15]. Kinetic fits and spectral simulations are described in **Supplementary Methods**.

Note: Supplementary information and chemical compound information is available on the Nature Chemical Biology website.

ACKNOWLEDGMENTS

E.R. Strieter is gratefully acknowledged for a generous gift of (*R,R*)-(−)-pseudoephedrine glycinamide hydrate. We thank F.H. Vaillancourt and J.A. Read for careful proofreading of the manuscript. This work was supported by the US National Institutes of Health (NIH GM-69657 to J.M.B. and C.K.; GM-20011 and GM-49338 to C.T.W.), the donors of the American Chemical Society Petroleum Research Fund (ACS-PRF 41170-G3 to C.K.), the Arnold and Mabel Beckman Foundation (Young Investigator Award to C.K.) and the Dreyfus Foundation (Camille Dreyfus Teacher Scholar Award to C.K.). D.P.G. is supported by the Damon Runyon Cancer Research Foundation Postdoctoral Fellowship (DRG-1893-05).

AUTHOR CONTRIBUTIONS

D.P.G., C.T.W., J.M.B. and C.K. designed the experiments and wrote the manuscript. D.P.G. overproduced and purified proteins, synthesized deuterated substrate, and performed iron titration and SF absorption experiments. D.P.G. and E.W.B. performed FQ experiments. C.K. collected and analyzed Mössbauer spectra.

COMPETING INTERESTS STATEMENT

The authors declare that they have no competing financial interests.

Published online at http://www.nature.com/naturechemicalbiology
Reprints and permissions information is available online at http://npg.nature.com/reprintsandpermissions

1. Gribble, G.W. Naturally occurring organohalogen compounds. *Acc. Chem. Res.* **31**, 141–152 (1998).
2. van Pee, K.-H. & Unversucht, S. Biological dehalogenation and halogenation reactions. *Chemosphere* **52**, 299–312 (2003).
3. Butler, A. & Carter-Franklin, J.N. The role of vanadium bromoperoxidase in the biosynthesis of halogenated marine natural products. *Nat. Prod. Rep.* **21**, 180–188 (2004).
4. Gribble, G.W. Natural organohalogens: a new frontier for medicinal agents? *J. Chem. Educ.* **81**, 1441–1449 (2004).
5. Fenical, W. & Jensen, P.R. Developing a new resource for drug discovery: marine actinomycete bacteria. *Nat. Chem. Biol.* **2**, 666–673 (2006).
6. Vaillancourt, F.H., Yin, J. & Walsh, C.T. SyrB2 in syringomycin E biosynthesis is a nonheme Fe^{II} α-ketoglutarate- and O_2-dependent halogenase. *Proc. Natl. Acad. Sci. USA* **102**, 10111–10116 (2005).
7. Vaillancourt, F.H., Yeh, E., Vosburg, D.A., Garneau-Tsodikova, S. & Walsh, C.T. Nature's inventory of halogenation catalysts: oxidative strategies predominate. *Chem. Rev.* **106**, 3364–3378 (2006).
8. Galonić, D.P., Vaillancourt, F.H. & Walsh, C.T. Halogenation of unactivated carbon centers in natural product biosynthesis: trichlorination of leucine during barbamide biosynthesis. *J. Am. Chem. Soc.* **128**, 3900–3901 (2006).
9. Vaillancourt, F.H., Yeh, E., Vosburg, D.A., O'Connor, S.E. & Walsh, C.T. Cryptic chlorination by a non-haem iron enzyme during cyclopropyl amino acid biosynthesis. *Nature* **436**, 1191–1194 (2005).
10. Ueki, M. *et al.* Enzymatic generation of the antimetabolite γ,γ-dichloroaminobutyrate by NRPS and mononuclear iron halogenase action in a Streptomycete. *Chem. Biol.* **13**, 1183–1191 (2006).
11. Solomon, E.I. *et al.* Geometric and electronic structure/function correlations in non-heme iron enzymes. *Chem. Rev.* **100**, 235–349 (2000).
12. Hausinger, R.P. Fe(II)/α-ketoglutarate-dependent hydroxylases and related enzymes. *Crit. Rev. Biochem. Mol. Biol.* **39**, 21–68 (2004).
13. Costas, M., Mehn, M.P., Jensen, M.P. & Que, L., Jr. Dioxygen activation at mononuclear nonheme iron active sites: enzymes, models, and intermediates. *Chem. Rev.* **104**, 939–986 (2004).
14. Hanauske-Abel, H.M. & Günzler, V. A stereochemical concept for the catalytic mechanism of prolylhydroxylase. Applicability to classification and design of inhibitors. *J. Theor. Biol.* **94**, 421–455 (1982).
15. Price, J.C., Barr, E.W., Tirupati, B., Bollinger, J.M., Jr. & Krebs, C. The first direct characterization of a high-valent iron intermediate in the reaction of an α-ketoglutarate-dependent dioxygenase: a high-spin Fe(IV) complex in taurine/α-ketoglutarate dioxygenase (TauD) from *Escherichia coli*. *Biochemistry* **42**, 7497–7508 (2003).
16. Price, J.C., Barr, E.W., Glass, T.E., Krebs, C. & Bollinger, J.M., Jr. Evidence for hydrogen abstraction from C1 of taurine by the high-spin Fe(IV) intermediate detected during oxygen activation by taurine:α-ketoglutarate dioxygenase (TauD). *J. Am. Chem. Soc.* **125**, 13008–13009 (2003).
17. Bollinger, J.M., Jr. & Krebs, C. Stalking intermediates in oxygen activation by iron enzymes: motivation and method. *J. Inorg. Biochem.* **100**, 586–605 (2006).
18. Proshlyakov, D.A., Henshaw, T.F., Monterosso, G.R., Ryle, M.J. & Hausinger, R.P. Direct detection of oxygen intermediates in the non-heme Fe enzyme taurine/α-ketoglutarate dioxygenase. *J. Am. Chem. Soc.* **126**, 1022–1023 (2004).
19. Riggs-Gelasco, P.J. *et al.* EXAFS spectroscopic evidence for an Fe=O unit in the Fe(IV) intermediate observed during oxygen activation by taurine:α-ketoglutarate dioxygenase. *J. Am. Chem. Soc.* **126**, 8108–8109 (2004).
20. Price, J.C., Barr, E.W., Hoffart, L.M., Krebs, C. & Bollinger, J.M., Jr. Kinetic dissection of the catalytic mechanism of taurine:α-ketoglutarate dioxygenase (TauD) from *Escherichia coli*. *Biochemistry* **44**, 8138–8147 (2005).
21. Hoffart, L.M., Barr, E.W., Guyer, R.B., Bollinger, J.M., Jr. & Krebs, C. Direct spectroscopic detection of a C-H-cleaving high-spin Fe(IV) complex in a prolyl-4-hydroxylase. *Proc. Natl. Acad. Sci. USA* **103**, 14738–14743 (2006).
22. Blasiak, L.C., Vaillancourt, F.H., Walsh, C.T. & Drennan, C.L. Crystal structure of the non-haem iron halogenase SyrB2 in syringomycin biosynthesis. *Nature* **440**, 368–371 (2006).
23. Koehntop, K.D., Emerson, J.P. & Que, L., Jr. The 2-His-1-carboxylate facial triad: a versatile platform for dioxygen activation by mononuclear non-heme iron(II) enzymes. *J. Biol. Inorg. Chem.* **10**, 87–93 (2005).
24. Quadri, L.E.N. *et al.* Characterization of Sfp, a *Bacillus subtilis* phosphopantetheinyl transferase for peptidyl carrier protein domains in peptide synthetases. *Biochemistry* **37**, 1585–1595 (1998).
25. Pavel, E.G. *et al.* Circular dichroism and magnetic circular dichroism spectroscopic studies of the non-heme ferrous active site in clavaminate synthase and its interaction with α–ketoglutarate cosubstrate. *J. Am. Chem. Soc.* **120**, 743–753 (1998).
26. Krebs, C. *et al.* Rapid freeze-quench ^{57}Fe Mössbauer spectroscopy: monitoring changes of an iron-containing active site during a biochemical reaction. *Inorg. Chem.* **44**, 742–757 (2005).
27. Pestovsky, O. *et al.* Aqueous Fe^{IV}=O: spectroscopic identification and oxo-group exchange. *Angew. Chem. Int. Ed.* **44**, 6871–6874 (2005).
28. Ryle, M.J. *et al.* O_2- and α-ketoglutarate-dependent tyrosyl radical formation in TauD, an α-keto acid-dependent non-heme iron dioxygenase. *Biochemistry* **42**, 1854–1862 (2003).
29. Liu, P. *et al.* Oxygenase activity in the self-hydroxylation of (*S*)-2-hydroxypropylphosphonic acid epoxidase involved in fosfomycin biosynthesis. *J. Am. Chem. Soc.* **126**, 10306–10312 (2004).
30. Neese, F. Theoretical spectroscopy of model-nonheme $[Fe(IV)OL_5]^{2+}$ complexes in their lowest triplet and quintet states using multireference ab initio and density functional theory methods. *J. Inorg. Biochem.* **100**, 716–726 (2006).
31. Kojima, T., Leising, R.A., Yan, S. & Que, L., Jr. Alkane functionalization at nonheme iron centers. Stoichiometric transfer of metal-bound ligands to alkane. *J. Am. Chem. Soc.* **115**, 11328–11335 (1993).
32. Burzlaff, N.I. *et al.* The reaction cycle of isopenicillin *N* synthase observed by X-ray diffraction. *Nature* **401**, 721–724 (1999).